(1952).
(16) S. Bumble and J. M. Honig, *J. Chem. Phys.*, **33**, 424 (1960).
(17) J. J. McAlpin and R. A. Pierotti, *J. Chem. Phys.*, **41**, 68 (1964).
(18) S. K. Kim and B. K. Oh, *This Solid Films*, **2**, 445 (1968).
(19) S. Chang and H. Pak, *J. Korean Chem. Soc.*, **14**, 97 (1970).
(20) D. M. Young and A. D. Crowell, "Physical Adsorption of Gases", Butterworth, Washington, D. C. (1960).
(21) S. Chang, H. Pak, J. W. Lee and S. J. Park, *J. Korean Chem. Soc.*, **21**, 313 (1977).
(22) S. Chang, J. W. Lee, H. Pak and S. Chang, *J. Korean Chem. Soc.*, **22**, 78 (1978).
(23) S. H. Han, J. W. Lee, H. Pak and S. Chang, *Bull. Korean Chem. Soc.*, **1**, 117 (1980).
(24) S. J. Park, J. W. Lee, H. Pak and S. Chang, *Bull. Korean Chem. Soc.*, **2**, 56 (1981).
(25) G. D. Halsey Jr., *J. Chem. Phys.*, **16**, 931 (1948).
(26) T. L. Hill, *J. Chem. Soc.*, **15**, 767 (1947).
(27) M. H. Polley, W. D. Schaeffer and W. R. Smith, *J. Phys. Chem.*, **57**, 469 (1953).
(28) N. N. Avgul, A. V. Kieselev and I. A. Lygina, *Kolloid Zh.*, **23**, 396 (1961).
(29) W. R. Smith and D. G. Ford, *J. Phys. Chem.*, **69**, 3587 (1965).
(30) R. A. Beebe and D. M. Young, *J. Phys. Chem.*, **58**, 93 (1954).
(31) B. W. Davis and C. Pierce, *J. Phys. Chem.*, **70**, 1051 (1966).
(32) C. Pierce and B Ewing, *J. Amer. Chem. Soc.*, **84**, 4070 (1962).
(33) For example, see T. L. Hill, "Introduction to Statistical Thermodynamics," Chapter 14, P. 246, Addison–Wesley.

Molecular Dynamic Study of a Polymeric Solution (I). Chain-Length Effect

Young Seek Lee and Taikyue Ree†

Korea Advanced Institute of Science and Technology P. O. Box 150, Chongyangni, Seoul 131, Korea
(Received January 21, 1982)

Dynamic and equilibrium structures of a polymer chain immersed in solvent molecules have been investigated by a molecular dynamic method. The calculation employs the Lennard–Jones potential function to represent the interactions between two solvent molecules (SS) and between a constituent particle (monomer unit) of the polymer chain and a solvent molecule (CS) as well as between two non-nearest neighbor constituent particles of the polymer chain (CC), while the chemical bond for nearest neighbor constituent particles was chosen to follow a harmonic oscillator potential law. The correlation function for the SS, CS and CC pairs, the end-to-end distance square and the radius of gyration square were calculated by varying the chain length (=5, 10, 15, 20). The computed end-to-end distance square and the radius of gyration square were found to be in a fairly good agreement with the corresponding results from the random-flight model. Unlike earlier works, the present simulation result shows that the autocorrelation function of the radius of gyration square decays slower than that of the end-to-end distance square.

Introduction

Polymers have several properties (viscosity, dielectric relaxation, *etc.*) which are distinctly different from those of monomers and low molecular weight compounds. The molecular weight of a polymer may be varied almost continuously from low to high by changing the degree of polymerization. Moreover, an individual polymer molecule has nearly infinite conformations. Therefore, it is difficult to derive physical properties of polymer systems from an *ab initio* theory.

Recent development of high-speed and high-capacity computers makes it possible to study complicated systems such as polymeric systems. Several attempts have been made in the past to simulate polymeric systems. The simulations on polymeric systems may be done either by the Monte Carlo method[1-9] or by the molecular dynamic method.[10-12] In Verdier's Monte Carlo simulation,[7-9] a polymer molecule was represented by a chain of connected lattice points, the unconnected lattice points by the solvent molecules. The constituent particles (or atoms) of the polymer chain have to be moved to other lattice points by a kinetic rule. It has been, however, pointed out that the Verdier's result may depend on the specific model used.[13,14] Ceperly and Kalos[15] simulated the dynamics of a polymer chain immersed in solvent, subject to both internal polymer force and random fluctuating solvent force. The simulation was done by solving the Smoluchowski equation for the time-evolution of the polymer probability density. The Smoluchowski equation does not take into account the solvent structure and solute-solvent interaction. Such details may greatly influence the dynamics of the polymer. The present study was undertaken to examine the behavior of the polymer in solution by carrying out the molecular dynamic calculation,

by treating both polymer and solvent from molecular level.

The molecular dynamic method simulates the motion of a system by a numerical solution of Newton's equation of motion. This method was first used by Alder and Wainwright[16,17] for a hard-sphere fluid, and by Rahman[18] for a Lennard-Jones fluid. Since then, it was successfully applied to examine many physically interesting problems on dense fluid,[19,20] glass transition,[21,22] *etc.* Unlike the Monte Carlo method, the molecular dynamic method generates a dynamic history; hence, one can obtain informations on both static and dynamic properties.

Although the molecular dynamic method has been applied to many problems as mentioned above, there have been only three attempts[10-12] to simulate the dynamic properties of polymeric solutions. The first study was made by Rapaport.[10] In his model, the polymer is represented by a freely linked chain of hard-spheres, and the solvent by a hard-sphere fluid. The number density used by Rapaport corresponds to a low-density situation. The second study was carried out by Bishop, Kalos, and Frisch[11]. In their model, successive constituent particles in the plolymer chain are linked by a spring obeying a logarithmic potential which is highly anharmonic. The solvent is assumed to be a Lennard-Jones fluid. They employed chain lengths of 5 and 10 and simulated at the reduced number density ρ^* $(=\rho\sigma^3)=0.3$ and the reduced temperature T^* $(=kT/\varepsilon)=10$, where σ and ε are the parameters appearing in the Lennard-Jones potential. This condition corresponds to a low-density and high temperature situation. The third study was made by Bruns and Bansal.[12] In Bruns and Bansal's model the polymer was represented by a chain of particles connected with rigid bonds, and the solvent assumed to be a Lennard-Jones fluid. The simulation was done near the triple point of the Lennard-Jones system, *i.e.*, at $\rho^*=0.85$ and $T^*=0.719$ for chain length equal to 9.

Like the above mentioned works,[11-12] the present molecular dynamic calculation makes use of the Lennard-Jones pair potential function for a polymeric solution. However, the model used here differs in that the chemical bond was represented by a harmonic oscillator potential. Morever, we have employed a large number (5, 10, 15, 20) of chain lengths than that used by other workers in order to observe the effect of chain length on physical properties. Detailed description on the model will be given later.

Molecular Dynamic Method

Dynamic and static properties of the Lennard-Jones (LJ) fluid have been extensively investigated by Verlet.[23,24] In our study Verlet's integration algorithm was adapted to solve the relevant Newton's equation of motion for a system of N particles, confined in a periodic cubic box with volume V; Pairwise additivity of the intermolecular potential is assumed. If the configuration and momentum coordinates of the particles at time t are known, the classical trajectory of the i-th particle can be determined by solving

$$m_i\ddot{r}_i=\sum_{j\neq i}^{N}F_{ij}(t)$$

$$=-\sum_{j\neq i}^{N}\frac{\partial}{\partial r_i}u(r_{ij}),\quad i=1,2,\cdots\cdots,N \tag{1}$$

where m_i is the mass of the i-th particle, and F_{ij} is the force exerted by the j-th particle on the i-th at time t, and $u(r_{ij})$ is the intermolecular potential, and $r_{ij}=|r_i-r_j|$. Expressions for $u(r_{ij})$ in Eq. (1) are given in the next section. We approximate Eq. (1) by Verlet's explicit time-centered finitc-difference algorithm,

$$r_i(t+\Delta t)=2r_i(t)-r_i(t-\Delta t)$$
$$-\frac{(\Delta t)^2}{m_i}\sum_{j\neq i}^{N}\frac{\partial}{\partial r_i}u(r_{ij})+O(\Delta t^4) \tag{2}$$

and the velocity of the i-th particle is given by

$$v_i(t)=|r_i(t+\Delta t)-r_i(t)|/\Delta t \tag{3}$$

We use Eq. (2) recurrsively to generate the position of the i-th particle $r_i(t)$ (i=1,2, ……, N) starting from $t=0$, Δt, $2\Delta t$,……, where Δt is chosen to conserve the total energy of the system, *i.e.*, 10^{-14} sec. In order to reduce the contribution by the finite size of the sample, three-dimensional periodic boundary conditions is used.[23,24] Initially, all particles are placed at lattice points corresponding to a face centered cubic lattice structure, and the initial velocities are chosen to have Maxwellian distribution at a temperature under the condition that the total momentum of the system is equal to zero. Before starting the simulation, we selected N_p particles whose positions are in the neighbor of the center of the box, and define them as the members of the polymer chain. Then, the initial positions of constituent particles in the polymer chain are altered from the fcc structure so that the distance between two bonded particles equals the bond length. The first 1000 time-steps were excluded from the averaging procedure to wash out the dependence of computed properties on the initial conformation of the solvent molecules and the polymer molecule.

Polymer Solution Model

N_p particles of the polymer chain in Figure 1 are linked by N_p-1 springs obeying the harmonic oscillator-potential law,

$$u(r_{i,i+1})=k_f(|r_i-r_{i+1}|-r_{eq})^2,\quad i=1,2,\cdots\cdots,N_p-1 \tag{4}$$

where k_f is the force constant of the spring, and r_{eq} is the equilibrium distance of the spring, *i.e.*, the bond length. In the present work r_{eq} is chosen to be equal to the σ-parameter in the Lennard-Jones potential. The interaction potential between two particles of solvent-solvent (SS), chain-solvent (CS), and two non-bonded chain elements (CC) are given by the Lennard-Jones potential,

$$u(r_{ij})=4\varepsilon\left[\left(\frac{\sigma}{r_{ij}}\right)^{12}-\left(\frac{\sigma}{r_{ij}}\right)^{6}\right]\quad \text{if } r_{ij}\leq 2.62\sigma$$
$$=0\qquad\qquad\qquad\qquad\qquad\qquad \text{if } r_{ij}>2.62\sigma \tag{5}$$

where parameters ε and σ are chosen to be the same as those of methane.[25] (See Figure 1.) The input data used are summarized in Table 1. In the calculation four chains of N_p equal to 5, 10, 15, and 20 were used.

Results and Discussion

(1) *Pair Correlation Functions.* A basic correlation function describing a local molecular arrangement is the pair-correlation function $g(r)$. The equilibrium $g(r)$ is time-independent, and is related to the average number of particles $<n(r)>$ within a spherical shell between r and $r+\Delta r$, from a particle at origin:

$$g(r)=\frac{<n(r)>}{4\pi r^2 \Delta r \rho} \tag{6}$$

where ρ is the number density$(=(N_p+N_s)/V)$ of the system, where N_s is the number of solvent molecules (particles), the number of particles N being equal to N_s+N_p. We have calculated $g(r)$ grom Eq. (6) at a given density ρ. The quantity $n(r)$ was obtained by averaging $n(r)$ over all time-steps, *i.e.*, $<A>$ denotes the time averaged quantity by Eq. (7).

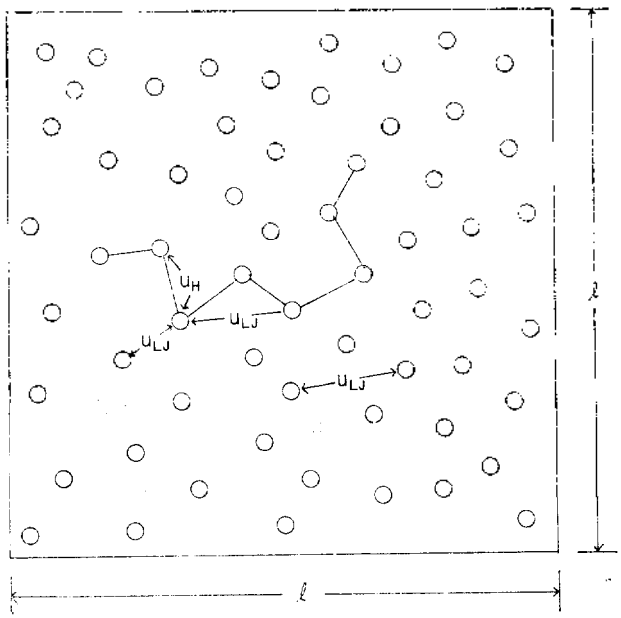

Figure. 1 Schematic representation of a polymer solution. Total number of particle: N is 108, and the polymer is composed of N_p constituent particles which are linearly connected by springs obeying a harmonic oscillator potential U_H, and all other inter-particle potentials are represented by the Lennard-Jones potential U_{LJ} as shown in the figure.

TABLE 1: Lennard-Jones Potential Parameters and the Data used in the Simulation

Quantity	Numerical value
density (ρ^*)	0.75
temperature	100 °K
time-step (Δt)	10^{-14} sec
σ	3.817×10^{-8} cm[a]
ϵ/k	148.2 °K[a]
$N(=N_s+N_p)$	108
mass	2.415×10^{-23} g
force constant k_f	1.97×10^5 dyne/cm[b]
total simulation steps	10^4 Δt

[a] Reference 26 p1111; [b] The k_f used in our calculation is similar to the k_f for butane, 1.54×10^5 dyne/cm.[27]

$$<A>=\frac{1}{n}\sum_{i=1}^{N} A(i\Delta t) \tag{7}$$

Note that there are three different pair correlation functions, corresponding to the solvent-solvent, chain-solvent, and chain-chain particle pairs. These correlation functions are denoted, respectively, by the SS $g(r)$, CS $g(r)$ and CC $g(r)$. These quantities obtained by our computations are shown in Figures. 2, 3, and 4, respectively. The positions and the heights of the first peak of the SS $g(r)$ and the CS $g(r)$ are given in Table 2. The SS $g(r)$'s, shown in Figure 2, have a form similar to the LJ $g(r)$.[27] In every case examined here, the positions of the first and second peaks occur at 1.12σ and 2.13σ, respectively. However, these peaks decrease with increasing chain length. In Figure 2 the total number of particle N is fixed, *i.e.*, $N=N_p+N_s$. This, in turn, reduces the coordination number of solvent molecules around a solvent molecules. However, the reduction in the first peak can be corrected by scaling the SS $g(r)$ by N/N_s, *i.e.*,

$$H'_{max}=H_{max}\cdot N/N_s \tag{8}$$

where H'_{max} and H_{max} are the corrected and uncorrected values for the first peak, respectively. Table 2 gives both H_{max} and H'_{max} at different N_p. We note that the above scaling relation, Eq. (8), makes H'_{max} insensitive to the variation of N_p (see the parenthesized data in Table 2). If we had used $\rho_s(=N_s/V)$ instead of $\rho(=N/V)$ in Eq. (6), as is done in the case of simple fluid mixtures,[28] the corresponding $g(r)$ would not have required such scaling procedure. In the

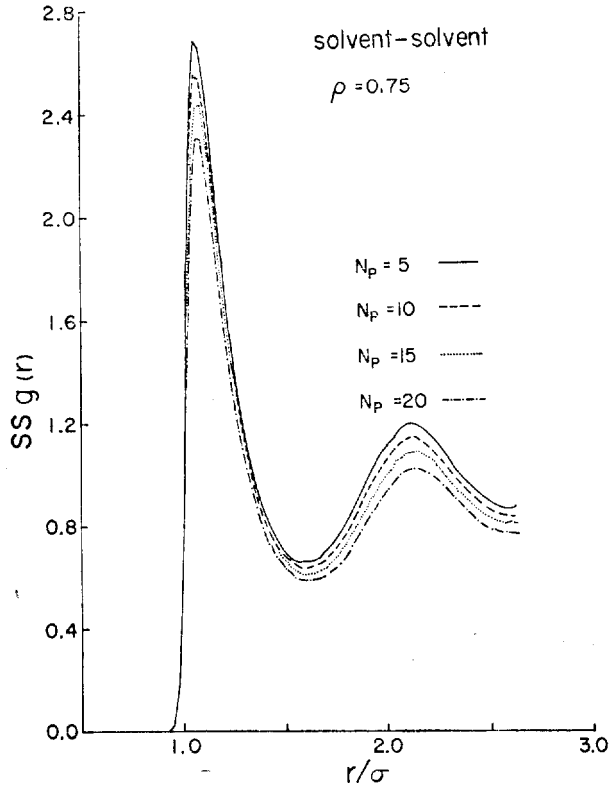

Figure. 2. Pair correlation function SS $g(r)$ for solvent-solvent in the polymeric solution at the reduced number density $\rho^*=0.75$. The first peak at 1.12σ corresponds to the first solvent molecular layer around a given solvent molecule, and the second peak at 2.13σ corresponds to the second solvent molecular layer around the solvent molecule.

limit of $N\to\infty$, however, no difference will occur between the two $g(r)$'s.

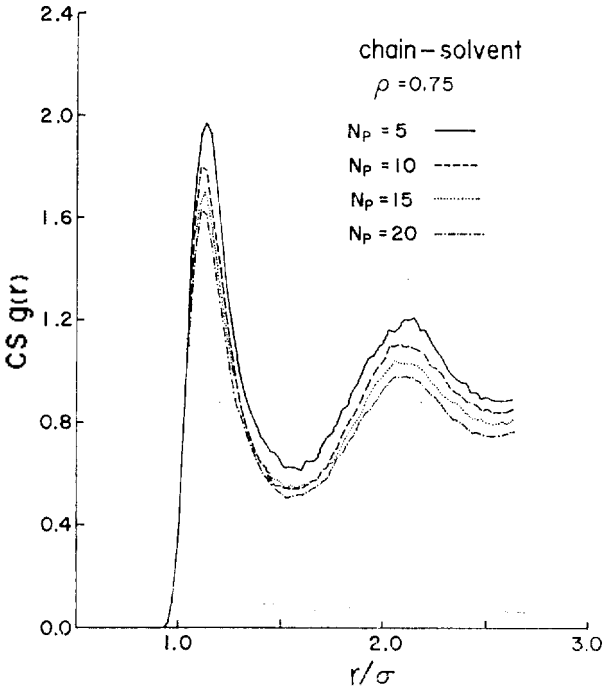

Figure 3. Pair correlation functions CS g(r) for chain–solvent in the polymeric solution at the reduced number density $\rho^*=0.75$. The unsmoothness of the curves compared to Figure 2 is caused by the fact $N_p \ll N_s$, *i. e.*, the process of averaging of $n(r)$ by N_p includes more statistical errors than in the SS $g(r)$. The first peak at 1.12σ corresponds to the first solvent molecular layer around a given constituent particle of the polymer chain, and the peak at 2.13σ corresponds to the second solvent molecular layer around the constituent particle.

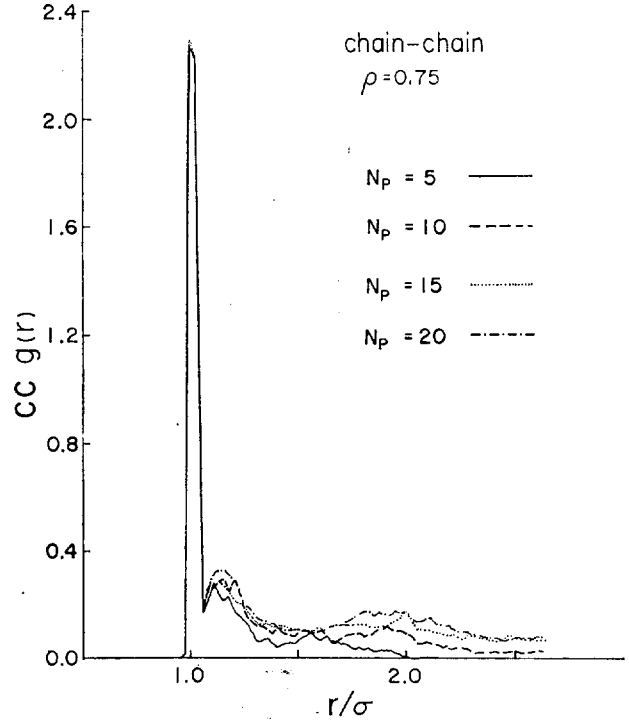

Figure 4. Pair correlation functions CC $g(r)$ for chain–chain at reduced number density $\rho^*=0.75$.

The CS $g(r)$ in Figure 3 exhibits a definite ordering of solvent molecules around a constituent chain particle. The CS $g(r)$ represent the probability density of solvent molecules which are at distance r from a constituent particle of the polymer chain. We note that the shape of the CS $g(r)$ is similar to that of the SS $g(r)$ in Figure 2. A minor irregularity in the CS $g(r)$ at $r/\sigma>1.5$ is due to a statistical uncertainty in computing the CS $g(r)$. Errors larger than that in the SS $g(r)$ occur because $N_p \ll N_s$. The first maximum lies a little lower than that in the SS g(r). This is expected on account of the fact that the neighbors of a constituent particle of the polymer chain are already occupied by the other constituent particles bonded directly to the former. Consequently, the probability of finding solvent molecules close to a constituent particle in the polymer chain is less than the probability of finding solvent molecules around another solvent molecule. The height of the second peak at a given N_p in the CS $g(r)$ in Figure 3 is almost equal to the corresponding peak of the SS $g(r)$ in Figure 2 irrespective of the chain-length differences. This means that the presence of a polymer can only weakly affect the distribution of solvent molecules if the solvent molecules lie at distance larger than corresponding to the first peak. The condition $\varepsilon_{CS}=\varepsilon_{SS}$ used in the simulation corresponds to a good solvent. This observation suggests that the second layer structure of the CS $g(r)$ for a real polymer in a good solvent will be nearly identical to that of bulk solvent.

We next turn our attention to the CC $g(r)$ which is related to the probability of finding constitutent particles of a polymer chain at distance r from a given constituent particle of the polymer. Figure 4 exhibits the CC $g(r)$'s at different values of N_p. Note that the CC $g(r)$ has a pronounced maximum at $r=\sigma$ which is equal to the bond length, linking the polymer chain. Furthermore, the shape of the first peak is not affected by the chain length except for the case $N_p=5$. For the latter case, the peak height of the CC $g(r)$ lies slightly lower (by about 1.2%) than the other cases (Figure 4). The difference, however, lies within the statistical uncertainty of the calculation. One significant feature in Figure 4 is the occurrence of a small peak at $r=1.12\sigma$. This distance corresponds to the potential minimum ($r_0=2^{1/6}\sigma$) of the L-J potential. Appearence of the peak here shows a small tendency of the polymer chain to form a cluster on account of the van der Waals attraction among the non-nearest neighbor constituent chain particles. Figure 4 shows still another peak

TABLE 2: The Heights and Positions of the First Peaks of Solvent-solvent and Chain-solvent Pair Correlation Functions

N_p	Solvent-solvent		Chain-solvent	
	Height	Position[a]	Height	Position[a]
5	2.68 (2.18)[b]	1.12	1.99 (2.09)[b]	1.12
10	2.56 (2.82)	1.12	1.80 (1.98)	1.12
15	2.43 (2.82)	1.12	1.71 (1.98)	1.12
20	2.31 (2.83)	1.12	1.63 (2.00)	1.12

[a] The length was given in σ units; [b] The data in parentheses are the corrected heights by using Eq. (8).

at $r \simeq 2\sigma$. The magnitude of the peak is much smaller than that of the first peak. Furthermore, it is sensitive to N_p. However, both larger system and larger time average than those used in this work are required to accurately pinpoint the exact nature of this peak. This require a formidable computing time which is beyond our resources. The broadness of the peak implies that the flexibility of the polymer chain beyond $r > 1.12\sigma$.

(2) *Configurational Properties of the Polymer Chain.* The spatial configuration of a polymer chain is characterized by the end-to-end distance square $R^2(t)$ and by the radius of gyration square $S^2(t)$, because the polymer chain moves continuously in solution by thermal motion. These quantity are defined by

$$R^2(t) = |\boldsymbol{r}_1(t) - \boldsymbol{r}_{N_p}(t)|^2 \tag{9}$$

and

$$S^2(t) = \frac{1}{N_p}\sum_{i=1}^{N_p} |\boldsymbol{r}_i(t) - \boldsymbol{r}_{cm}(t)|^2 \tag{10}$$

where $\mathbf{r}_{cm}$ is the center-of-mass vector of the polymer chain, defined by

$$\boldsymbol{r}_{cm}(t) = \frac{1}{N_p}\sum_{i=1}^{N_p} \boldsymbol{r}_i(t) \tag{11}$$

The quantities $\langle R^2 \rangle$ and $\langle S^2 \rangle$ were computed by averaging $R^2(t)$ and $S^2(t)$ over the molecular dynamic time-steps. The results are shown in columns 2 and 3 of Table 3, where the length was given in σ units. In the case of the freely jointed polymer model, $\langle R^2 \rangle$ and $\langle S^2 \rangle$ are given by[29,30]

$$\langle R^2 \rangle = nl^2 \tag{12}$$

and

$$\langle S^2 \rangle = \langle R^2 \rangle / 6 \tag{13}$$

where n and l are the number of bonds and bond length, respectively, *i.e.*, $n = N_p - 1, l = \sigma$ in terms of the present paper. Values of $\langle R^2 \rangle$ calculated from Eq.(9) agree satisfactorily with the values calculated from Eq. (12). (See Table 3.) It should also be noted that the *ratio* $\langle R^2 \rangle / \langle S^2 \rangle$ (see column 4 in Table 3) is approximately equal to the value (= 6) predicted by the random flight model Eq. (13). The aforementioned agreement between the present molecular dynamic simulation and the random flight model implies that the polymer chain in a good solvent may be approximated by a random coil, both in dilute solution as well as in highly concentrated solution, because the concentrations of the polymers corresponding to $N_p = 5$, 10, 15, and 20 are 4.63, 9.26, 13,89, and 18.52 wt. percent, respectively.

The moment of inertia tensor is defined by[31]

$$T_{ab}(t) = \frac{1}{N_p}\sum_{i=1}^{N_p} |\boldsymbol{r}_i(t) - \boldsymbol{r}_{cm}(t)|_a \cdot |\boldsymbol{r}_i(t) - \boldsymbol{r}_{cm}(t)|_b \tag{14}$$

where the subscripts a and b denote x,y, or z. The eigenvalues $S_1^2(t)$, $S_2^2(t)$, and $S_3^2(t)$ of tensor T (t) characterize the shape of the polymer chain, and $S^2(t)$ in Eq. (10) is related to $S_i^2(t)$ $(i = 1,2$ or $3)$ by

$$S^2(t) = S_1^2(t) + S_2^2(t) + S_3^2(t) \tag{15}$$

We have computed the time-averages $\langle S_i^2 \rangle$'s, and the results are tabulated in Table 3, where the $\langle S_i^2 \rangle$'s are normalized by dividing them by $\langle S^2 \rangle$. In the case of a chain with spherical shape, $\langle S_i^2 \rangle$'s are equal to 1/3; the departure from this value gives a measure of the asphericity in the distribution of the constituent particles of the chain. From the $\langle S_i^2 \rangle$ values in Table 3 we conclude that the equilibrium spatial configuration of the polymer has a shape of a distorted ellipsoid, and that the shape of the polymer is not altered in any noticeable way by the change in the chain length of the polymer.

(3) *Relaxation Propeties of Polymer Chain.* The chain relaxation is characterized by the decay of the autocorrelation functions of the end-to-end distance square and of the radius of gyration square,[32] *i.e.*,

$$C(t;A) = \frac{\langle A(t_0)A(t_0+t)\rangle - \langle A(t_0)\rangle^2}{\langle A^2(t_0)\rangle - \langle A(t_0)\rangle^2} \tag{16}$$

where A represents either $R^2(t)$ *or* $S^2(t)$. The autocorrelation function $C(t;A)$ means

TABLE 3: Chain Configurational Properties;Mean Square End-to-end Distance $\langle R^2 \rangle$, Mean Square Radius of Gyration $\langle S^2 \rangle$, and Mean Eigenvalues of the Monent of Inertia Tensor

N_p	$\langle R^2 \rangle^a$	$\langle S^2 \rangle^a$	$\langle R^2 \rangle / \langle S^2 \rangle$	$\langle S_1^2 \rangle^b$	$\langle S_2^2 \rangle^b$	$\langle S_3^2 \rangle^b$
5	4.75 (4)	0.856	5.55	0.235	0.356	0.409
10	12.12 (9)	1.746	6.99	0.200	0.400	0.400
15	15.35 (14)	2.936	5.22	0.232	0.329	0.439
20	18.90 (19)	3.352	5.64	0.209	0.342	0.449

[a] The length was given in σ units; [b] $\langle s_i^2 \rangle$'s (i=1, 2, 3) were normalized by divding by $\langle S^2 \rangle$; [c] The data in parentheses were calculated from Eq. (12).

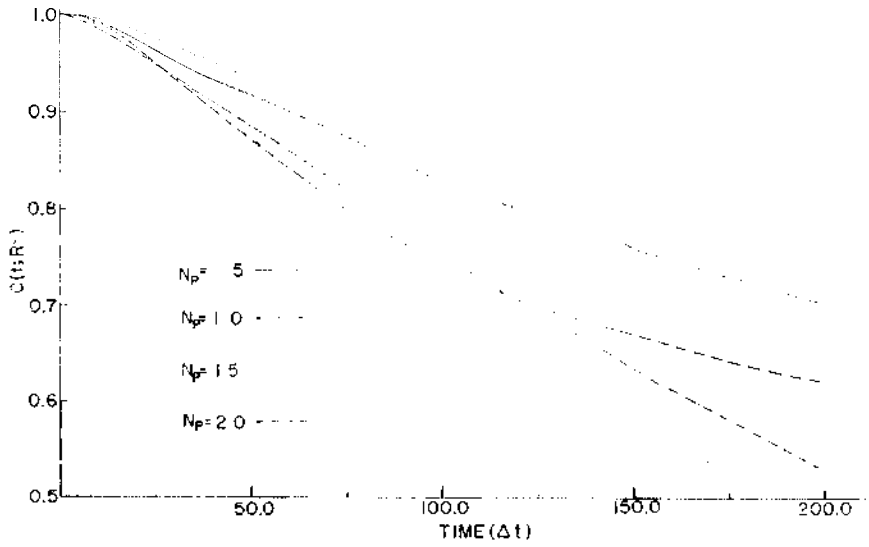

Figure 5. Autocorrelation function of the end-to-end distance square. The time axis is shown in units of Δt.

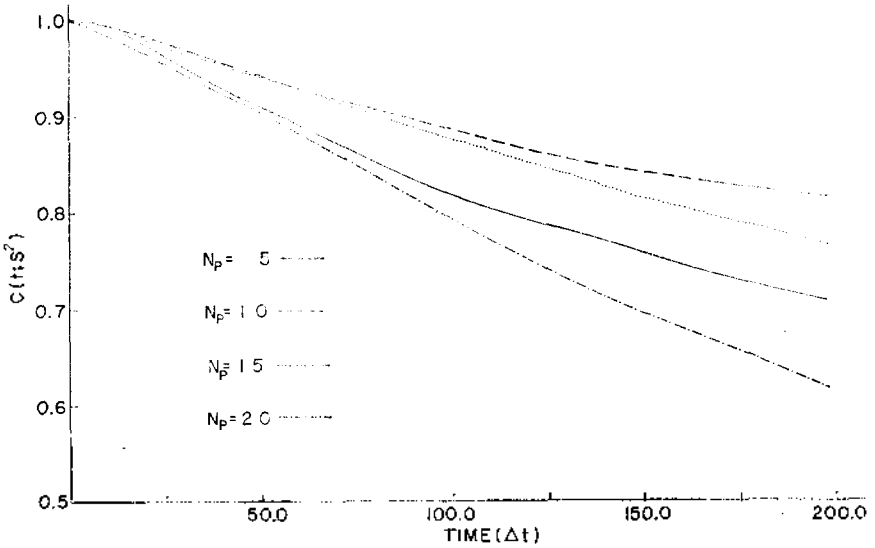

Figure 6. Autocorrelation function of the radius of gyration square. The time axis is shown in units of Δt.

the extent to which a configuration at time t_0 influences the configuration at a later time t_0+t. We have calculated $C(t;R^2)$ and $C(t;S^2)$ using *Eq.* (16), and the results are shown in Figure. 5 and 6, respectively. Actual calculation were performed up to 2000 time-steps, but only the results to 200 time-steps are shown in Figures 5 and 6 since beyond the 200 time-step the $C(t;A)$ oscillates. We note that $C(t;R^2)$ and $C(t;S^2)$ vary irregularly with the chain lengths. However, the decay of $C(t;S^2)$ is seen to be generally slower than $C(t;R^2)$. This result differs from the works of earlier workers. Namely, Rapaport[10] concluded that the decay of $C(t;S^2)$ is approximately equal to that of $C(t;S^2)$, whereas Bishop et al.[11] and Bruns and Bansal[12] concluded that $C(t;R^2)$ decays slower than $C(t;S^2)$. Since $R^2(t)$ was determined by the two-end constituent particles in the particles in the polymer [See Eq. (9)] and $S^2(t)$ by N_p positions of the constituent particles [See Eq. (10)], it is reasonable to expect that the fluctuation in $S^2(t)$ is smaller than that in $R^2(t)$. Consequently, one may expect that $C(t;S^2)>C(t;R^2)$, in turn, the former decays slower than the latter. This argument supports the present simulation result which shows $C(t;S^2)$ to decay slower than $C(t;R^2)$.

Acknowledgement. We are deeply indebted to Dr. Francis H. Ree and Professor J. J. Kim for their valuable discussions and advices. We also acknowledge the Korea Research Center for Theoretical Physics and Chemistry for a partial support of this work.

Reference

(1) K. Iwata and M. Kurata, *J. Chem. Phys.*, **50,** 4008 (1969).
(2) R. Grishman, *J. Chem. Phys.*, **58,** 220 (1972).
(3) J. Mazur, C. M. Guttman, and F. L. McCrackin, *Macromolecules,* **6,** 872 (1973).
(4) P. G. De Gennes, *Macromolecules,* **9,** 587 (1976).
(5) D. E. Kranbuehl and P. H. Verdier, *J. Chem. Phys.*, **67,** 361 (1977).
(6) A Baumgartner, *J. Chem. Phys*, **72,** 871 (1980).
(7) P. H. Verdier and W. H. Stockmayer, *J. Chem. Phys.*, **36,** 227 (1962).
(8) P. H. Verdier, *J. Chem. Phys.*, **45,** 2118 (1966).
(9) P. H. Verdier, *J. Chem. Phys.*, **45,** 2122 (1966).
(10) D. C. Rapaport, *J. Phys.*, **All,** L213 (1978); *J. Chem. Phys.*, **71,** 3299 (1980).
(11) M. Bishop, M. H. Kalos and H. L. Frisch, *J. Chem., Phys* **70,** 1299 (1979).
(12) W. Bruns and R. Bansal, *J. Chem. Phys.*, **74,** 2064 (1981).
(13) H. J. Hilhorst and J. M. Deutch, *J. Chem. Phys.*, **63,** 5153 (1975).
(14) H. Boots and J. M. Deutch, *J. Chem. Phys.*, **67,** 4608 (1977).
(15) D. Ceperley and M. H. Kalos, Phys. Rev. Letters, **41,** 313 (1978).
(16) B. J. Alder and T. E. Wainwright, *J. Chem. Phys.*, **31,** 459 (1959).
(17) B. J. Alder and T. E. Wainwright, *J. Chem. Phys.*, **33,** 1439 (1960).
(18) A Rahman, *Phys. Rev.*, **136A,** 405 (1964).
(19) J. J. Weis and D. Levesque, *Phys. Rev.*, **A13,** 450 (1976).
(20) J. P. J. Michels and N. J. Trappeniers, *Physica,* **90A,** 179 (1978).
(21) A Rahman, M. J. Mandell and J. P. McTague, *J. Chem. Phys.*, **64,** 1564 (1976).
(22) J. N. Cape and L. V. Woodcock, *J. Chem. Phys.*, **72,** 966 (1980).
(23) L. Verlet, *Phys. Rev.*, **159,** 98 (1967).
(24) L. Verlet, *Phys. Rev.*, **165,** 201 (1968).
(25) J. O. Hirschfelder, C. F. Curtiss and R. B. Bird, "Molecular Theory of Gases and Liquids," p. 1111, John Wiley & Sons Inc., New York, 1964.
(26) T. A. Weber, *J. Chem. Phys.*, **69,** 2347 (1978).
(27) K. Toukubo and K. Nakanishi, *J. Chem. Phys.*, **65,** 1937 (1976).
(28) T. M. Reed and K. E. Gubbins, "Applied Statistical Mechanics," McGraw-Hill, New York, 1973, Chapter 6.
(29) H. Yamakawa, "Modern Theory of Polymer Solutions," Harper and Row Publisher, New York, 1971, Chapter 2.
(30) P. J. Flory, "Statistical Mechanics of Chain Molecules," Interscience Publishers, New York, 1969, Chapter 1.
(31) K. Sŏlc, *J. Chem. Phys.*, **55,** 335 (1971).
(32) G. E. P. Box and G. M. Jenkins, "Time Series Analysis Forecasting and Control," p. 28, Holden-day, San Francisco, 1970.